Ex vivo culture of circulating breast tumor cells for individualized testing of drug susceptibility

Ex Vivo Culture of Circulating Breast Tumor Cells for Individualized Testing of Drug Susceptibility

Min Yu [1,7 #], Aditya Bardia[1,3], Nicola Aceto[1,3], Francesca Bersani[1,3], Marissa W. Madden[1,3], Maria C. Donaldson[1,3], Rushil Desai[1,3], Huili Zhu[1], Valentine Comaills[1,3], Zongli Zheng[1,4,8], Ben S. Wittner[1,3], Petar Stojanov[6], Elena Brachtel[4], Dennis Sgroi[1,4], Ravi Kapur[2], Toshihiro Shioda[1,3], David T. Ting [1,3], Sridhar Ramaswamy [1,3], Gad Getz[1,4, 6], A. John Iafrate[1,4], Cyril Benes[1, 3], Mehmet Toner[2,5], Shyamala Maheswaran [1,5 *] Daniel A. Haber [1,3,7 *].

[1] Massachusetts General Hospital Cancer Center, [2] Center for Bioengineering in Medicine, and Departments of [3] Medicine, [4] Pathology, [5] Surgery, Harvard Medical School, Charlestown, MA 02129

[6] Broad Institute of Harvard and MIT, Cambridge, MA 02142

[7] Howard Hughes Medical Institute, Chevy Chase, MD 20815

[8] Department of Medical Epidemiology and Biostatistics, Karolinska Insitutet, Stockholm, Sweden

Current address: Department of Stem Cell Biology and Regenerative Medicine, University of Southern California, Los Angeles, CA 90033

[*] To whom correspondence should be addressed. E-mail: Maheswaran@helix.mgh.harvard.edu and Haber@helix.mgh.harvard.edu

Abstract:

Circulating tumor cells (CTCs) are present at low levels in the peripheral blood of patients with solid tumors. It has been proposed that the isolation, *ex vivo* culture, and characterization of CTCs may provide an opportunity to noninvasively monitor the changing patterns of drug susceptibility in individual patients as their tumors acquire new mutations. In a proof-of-concept study, we established CTC cultures from six patients with estrogen receptor-positive breast cancer. Three of five CTC lines tested were tumorigenic in mice. Genome sequencing of the CTC lines revealed pre-existing mutations in the *PIK3CA* gene and newly acquired mutations in the estrogen receptor gene (*ESR1*), *PIK3CA* gene and the fibroblast growth factor receptor gene (*FGFR2*), among others. Importantly, drug sensitivity testing of CTC lines with multiple mutations revealed potential new therapeutic targets. With optimization of CTC culture conditions, this strategy may help identify the best therapies for individual cancer patients over the course of their disease.

Main Text:

Circulating tumor cells (CTCs) are present in the blood of many patients with solid tumors. The majority of these cells, which are thought to be involved in metastasis, die in the circulation, presumably due to the loss of matrix-derived survival signals or circulatory shear stress. Nonetheless, if CTCs can be isolated from cancer patients as viable cells that can be genotyped and functionally characterized over the course of therapy, they have the potential to identify treatments that most effectively target the evolving mutational profile of the primary tumor (*1*). The isolation of viable CTCs is technically challenging: most methods yield low numbers of partially purified CTCs that are fixed prior to isolation, damaged during the cell purification process, or irreversibly immobilized on an adherent matrix (see review (*2*)). We recently reported a microfluidic technology, the CTC-iChip, which efficiently depletes normal blood cells, leaving behind unmanipulated CTCs (*3*). The cytological appearance, staining properties and intact RNA evident within a subset of CTCs isolated using this tumor antigen-agnostic CTC isolation platform, suggested that the cells may be viable.

To investigate whether the CTCs were in fact viable, we applied the CTC-iChip to blood samples from patients with metastatic estrogen receptor (ER)-positive breast cancer. After testing a range of culture conditions (*4-7*) (see supplementary method), we found that CTCs proliferated best as tumor spheres when cultured in serum-free media supplemented with epidermal growth factor (EGF) and fibroblast growth factor basic (FGFb) (*8*) under hypoxic conditions (4% O_2) (Fig. 1A). Non-adherent culture conditions were critical, since CTCs senesced after a few cell divisions in adherent monolayer culture (Fig. S1). We established long-term oligoclonal CTC cultures

(sustained *in vitro* for > 6 months) from CTCs isolated from six patients with metastatic luminal subtype breast cancers (Table S1). One or more CTC cell lines were successfully generated from six of 36 patients who were either off therapy or progressing on treatment. We were unable to generate CTC cell lines from nine patients who were responding to treatment at the time of attempted CTC culture. For three patients, four additional CTC cell lines were established from blood samples drawn at multiple different time points during therapy (Table S1). In these cases, CTCs were successfully cultured only when patients were progressing on treatment (Fig. S1).

Cultured CTCs shared cytological features with the matched primary CTCs captured on the CTC-iChip (Fig. 1A), and consistent with standard CTC definitions, they stained positive for epithelial cytokeratin (>95% of cells) and negative for the leukocyte marker CD45 (Fig. 1A) (Fig. S2). The proliferative index of CTC cultures was approximately 30%, as defined by Ki67 staining (mean 28.1%, range 24-32%), and the initial doubling time of CTC cultures varied from 3 days to 3 weeks (Table S1). All six primary tumors were positive for ER expression. Five CTC lines retained ER positivity in culture (>10% of cells), while one line (BRx-07) lost ER expression *in vitro* (Fig. 1C) (Fig. S2).

We undertook RNA sequencing analysis of each cell line and compared the results with 29 uncultured single CTCs from a total of 10 patients as well as a panel of 13 commonly used established breast cancer cell lines, all using low template single cell resolution analysis (Fig. S3). CTC cultures clustered with each other, and separately from established breast cancer cell lines or uncultured single CTCs. As expected, both CTC cultures and established breast cancer cell

lines had elevated proliferative signatures, compared with primary uncultured single CTCs (Fig. S3). We did not observe increased expression in CTC cultures of defined signaling pathways, including stem cell-related signatures, compared with established breast cancer cell lines.

To test the tumorigenicity of CTC lines, we used lentiviral transduction to label them with both green fluorescent protein (GFP) and luciferase and inoculated 20,000 cells into the mammary fat pad of immunosuppressed non-obese diabetic *scid* gamma (NSG) female mice implanted with subcutaneous estrogen pellets. Of five CTC lines tested, three (BRx-07, BRx-68 and BRx-61) generated tumors within 3 months at this low inoculum (Fig. 1B) (Fig. S4-5). CTC-derived tumors shared histological and immunohistochemical features with the matched primary patient tumor, including BRx-07, which regained ER expression (Fig. 1C).

All six patients with metastatic breast cancer had received sequential courses of hormonal and other therapies prior to CTC collection (Fig. S6). As part of standard clinical care at Massachusetts General Hospital, a mutational panel (SNaPShot, (*9*)) covering approximately 140 mutations in 25 genes had been performed on primary tumor specimens (BRx-68 and BRx-42) or on pre-treatment biopsies of metastatic lesions (BRx-33, BRx-07, BRx-50 and BRx-61). Point mutations in *PIK3CA* (H1047R and G1049R), hot spot mutations in breast cancer, were identified in 2 cases (BRx-68 and BRx-42), while no mutations were found in the four other cases (Table S1). The availability of CTC cultures made it possible to undertake more comprehensive mutational analysis from a more abundant and purified tumor cell population. CTC lines were screened for mutations in a panel of 1,000 annotated cancer genes, using a

hybrid-capture-based next generation sequencing (NGS) platform. The *PIK3CA* mutations identified by SNaPShot testing of primary tumors were confirmed by NGS in both CTC cultures (BRx-68 and BRx-42), and multiple additional mutations in other cancer-related genes were identified (Table 1). For all mutations identified in the 1,000 cancer gene panel, candidate driver mutations were defined by their absence from matched germline DNA and by their annotation in pan-cancer (*10*) and COSMIC databases (Table 1), while additional mutations in known cancer genes were of uncertain significance (Table S2). To ensure that the candidate driver mutations were not acquired during the *in vitro* establishment of CTC cell lines, we tested for selected mutations in four additional CTC lines, which had been independently isolated at different time points from each of three patients (BRx-68, BRx-42, and BRx-61). The acquired mutations in *ESR1* (BRx-68), *TP53* (BRx-68, BRx-61), *KRAS* (BRx-42) were universally present in all independent CTC cell lines (Table 1), confirming that they are tumor-derived mutations. In addition, the *ESR1* mutation (Y537S) present in multiple BRx-68 CTC lines was also detectable by direct RNA sequencing of uncultured CTCs isolated from this patient (Fig. S7).

Activating mutations in the estrogen receptor (*ESR1*) were first identified in 1997 and are rare in primary breast cancer (*11*). While this manuscript was in preparation, multiple research groups reported *ESR1* mutations in 18-54% of patients treated with aromatase inhibitors (AIs), drugs that suppress estrogen synthesis and thus may favor the emergence of these ligand-independent estrogen receptor mutants (*12*-*15*). We also detected *ESR1* mutations in 3/6 CTC lines (BRx-33, BRx-68, and BRx-50). Each of these patients had received extensive treatment with AIs, and reanalysis of the primary tumor or the pre-AI treatment biopsy of a metastatic lesion showed no evidence of *ESR1* mutations (Table 1). Other mutations identified included newly arising

mutations in *PIK3CA*, *TP53*, *KRAS* and Fibroblast Growth Factor Receptor-2 (*FGFR2*) (Table 1). Consistent with its lobular histological subtype, an E-cadherin (*CDH1*) mutation was detected in one CTC line (BRx-07). While most mutant allele frequencies indicated heterozygous or homozygous truncal mutations shared by all CTCs, rare mutated alleles consistent with emerging tumor subpopulations were also evident. An *ESR1* mutation initially present at 6% allele frequency in BRx-50 increased to 49% allele frequency upon prolonged culture in low-estrogen containing medium (Table 1), suggesting a proliferative advantage under these conditions. Interestingly, *TP53* mutations, which are thought to be rare in primary luminal breast cancers (*16*), emerged during tumor progression in three of six cases.

The availability of comprehensive tumor cell genotyping brings with it the challenge of identifying the subset of mutations whose therapeutic targeting is likely to be beneficial to an individual patient. To begin to explore this opportunity, we tested CTC lines for sensitivity to panels of single drug and drug combinations, including standard clinical regimens, as well as experimental agents targeting specific mutations. Conditions were optimized for highly reproducible testing of viability in small numbers of cells (200 cells/well) cultured as aggregates in solution. For each drug, we tested five concentrations (Table S3), centered around IC_{50} levels established in large-scale cancer cell line screens (*17*), with relative sensitivity or resistance defined by comparison among the CTC cell lines (Fig. 2) (Figs. S8-10). While CTC drug sensitivity testing was blinded to clinical history, and patient treatment selections were not informed by CTC testing, we note that some CTC drug sensitivity measurements were concordant with clinical histories, including sensitivity to paclitaxel (BRx-07) and to

capecitabine (BRx-68 and BRx-50), and resistance to fulvestrant (BRx-07, BRx-68), to doxorubicin (BRx-07) and to olaparib (BRx-50) (Fig. S11).

We selected two mutated drug targets identified in CTCs but not in the primary tumor for more detailed analysis, namely *ESR1* and *PIK3CA* mutations (additional drug responses in cultured CTCs are shown in supplementary Fig. S12). To facilitate interpretation of the effect of drug combinations, responses to selected drugs are represented in a 2x2 matrix highlighting cooperative drug effects versus independent cytotoxicity (Fig. 3; see quantitation in Fig. S13). The three *de novo* acquired *ESR1* mutations affected distinct but adjacent residues within the ER ligand binding domain, and were present at different allele frequencies within the oligoclonal CTC cell lines. The most commonly reported *ESR1* mutation, Y537S (*12-14*), was observed in BRx-68 (47% allele frequency, consistent with a heterozygous mutation in all cells), with two other mutations, D538G and L536P, in BRx-33 and BRx-50 (24% and 6% allele frequencies, respectively). Each mutation arose within the context of distinct additional mutations (Table 1) (Table S2). Of note, all *ESR1* mutation-positive CTC lines maintained expression of the estrogen receptor in culture.

The optimal therapy for breast cancer patients whose ER+ tumor has acquired an *ESR1* mutation is unknown: consistent with previous models (*12-14, 18*), we found that the selective estrogen receptor modulators (SERM) tamoxifen and raloxifene, and the selective ER degrader (SERD) fulvestrant were ineffective in BRx-68 cells, either alone or in the clinically approved combination with inhibitors of the PI3K/mTOR pathway (everolimus) (*19*) (Fig. 2). However,

the HSP90 inhibitor STA9090 demonstrated cytotoxicity alone, and in combination with both raloxifene and fulvestrant (Fig. 3A). ER is a client protein for HSP90 and mutated receptors are highly dependent on this chaperone for their stability (*20*). Indeed, treatment with a low dose of STA9090 (32nM) suppressed ER levels in BRx-68 cells, but had no effect in MCF7 breast cancer cells with wild type ER, or in BRx-50 cells, where the low allele frequency of mutant *ESR1* is not associated with sensitivity to HSP90 inhibitors (Fig. 3B) (Fig. S12-14). Clinical studies of HSP90 inhibitors, along with novel ER inhibitors will be required to define the optimal treatment for breast cancer patients whose tumor has acquired an *ESR1* mutation.

The BRx-07 cell line is noteworthy because it harbors activating mutations in both *PIK3CA* and *FGFR2*, both of which were acquired *de novo* during the course of therapy. Based on their respective allele frequencies, *PIK3CA* was homozygously mutated in all cells, whereas the *FGFR2* mutation was heterozygous (Table 1). Cultured CTCs were highly sensitive to the PIK3CA inhibitor BYL719 (*21*), and the FGFR2 inhibitor AZD4547 (*22*), and moderately responsive to the FGFR1 inhibitor PD173074 (*23*) (Fig. 2). Combined inhibition of both PIK3CA and FGFR2 showed cooperative effects (Fig. 3C) (Fig. S13), suggesting that both of these mutations may function as acquired oncogenic drivers in this tumor. Since combinations of PIK3CA and FGFR inhibitors have not been tested in clinical settings, we further quantified responses in a panel of established breast cancer cell lines. Of seven *PIK3CA*-mutant breast cancer lines, six were responsive to BYL719 (Fig. S15). Interestingly, in addition to their characteristic *PIK3CA* mutation, two lines harbored mutations of unkown significance in *FGFR4* (Y367C; MDA-MB-453 cells) and in *FGFR2* (K570E; EFM-19 cells). The former showed cooperative cytotoxicity by BYL719 and AZD4547, while the latter was insensitive to FGFR

inhibition (Fig. S15). One of five *PIK3CA*-mutant breast cancer lines without an FGFR gene mutation showed modest sensitivity to AZD4547 (CAL51), while the other four were resistant. Thus, the combination of genotyping and functional testing for drug susceptibility is essential to defining therapeutically relevant driver mutations in both breast cancer cell lines and CTC cultures.

In vitro screening of additional drugs for cooperation with PIK3CA-targeted agents identified inhibitors of the insulin-like growth factor receptor 1 (*IGF1R*, inhibitors OSI906 and BMS754807) and HSP90 (inhibitor STA9090, Ganetespib) (Fig. 3C). While neither of these is mutated in BRx-07 cells, IGF1R has been implicated in modulating signaling loops that mitigate sensitivity to PI3K inhibitors (*24*), and HSP90 is involved in stabilization of mutant kinases (*20*). To extend drug sensitivity studies to mouse xenografts, we generated BRx-07-derived mammary tumors, and treated these with BYL719, AZD4547, the two agents in combination, or diluent control. *In vivo* tumor suppression was observed following treatment with either drug individually, whereas the combination completely abrogated tumor growth (Fig. 3D).

In summary, in this proof-of-concept study, we have shown that the culture of tumor cells circulating in the blood of patients with breast cancer provides an opportunity to study patterns of drug susceptibility, linked to the genetic context that is unique to an individual tumor. In patients with hormone-responsive breast cancer, most of whom have bone metastases that are not readily biopsied, the ability to noninvasively and repeatedly analyze live tumor cells shed into the blood from multiple metastatic lesions may enable monitoring of emerging subclones with

altered mutational and drug sensitivity profiles. The successful culture of CTCs stems in part from the application of a microfluidic device capable of effectively depleting leukocytes from a blood specimen while preserving viable tumor cells for *ex vivo* expansion (*3*). The proliferation of cultured CTCs as non-adherent spheres differs from that of characteristic epithelial cancer cell cultures and may reflect intrinsic properties of tumor cells that remain viable in the bloodstream, following loss of attachment to basement membrane. A recent report documented direct inoculation of the mouse femur with blood-derived cancer cells from a patient who had very high numbers of CTCs, but *in vitro* culture was not successful (*25*). Our results differ from the adherent *in vitro* CTC cultures described by Zhang et al (*26*), but these lines appear to share the identical *TP53, BRAF* and *KRAS* genotype of the highly tumorigenic MDA-MB-231 cell line.

Importantly, optimization of CTC culture conditions will be needed before this strategy can be incorporated into clinical practice. In addition, further characterization of the non-adherent CTC-derived cell lines described here will be required to define how they differ from cells cultured from primary tumor biopsies or directly implanted into mouse models (*4, 14*). In the future, strategies such as that described here may be an essential component of "precision medicine" in oncology, where treatment decisions are based on evolving tumor mutational profiles and drug sensitivity patterns in individual patients.

References:

1. D. A. Haber, N. S. Gray, J. Baselga, *Cell* **145**, 19 (Apr 1, 2011).
2. M. Yu, S. Stott, M. Toner, S. Maheswaran, D. A. Haber, *J Cell Biol* **192**, 373 (Feb 7, 2011).
3. E. Ozkumur *et al.*, *Sci Transl Med* **5**, 179ra47 (Apr 3, 2013).
4. X. Liu *et al.*, *Am J Pathol* **180**, 599 (Feb, 2012).
5. T. Sato, H. Clevers, *Methods Mol Biol* **945**, 319 (2013).
6. T. A. Ince *et al.*, *Cancer Cell* **12**, 160 (Aug, 2007).
7. J. Debnath, S. K. Muthuswamy, J. S. Brugge, *Methods* **30**, 256 (Jul, 2003).
8. G. Dontu *et al.*, *Genes Dev* **17**, 1253 (May 15, 2003).
9. D. Dias-Santagata *et al.*, *EMBO Mol Med* **2**, 146 (May, 2010).
10. M. S. Lawrence *et al.*, *Nature* **505**, 495 (Jan 5, 2014).
11. Q. X. Zhang, A. Borg, D. M. Wolf, S. Oesterreich, S. A. Fuqua, *Cancer Res* **57**, 1244 (Apr 1, 1997).
12. D. R. Robinson *et al.*, *Nat Genet* **45**, 1446 (Dec, 2013).
13. W. Toy *et al.*, *Nat Genet* **45**, 1439 (Dec, 2013).
14. S. Li *et al.*, *Cell Rep* **4**, 1116 (Sep 26, 2013).
15. K. Merenbakh-Lamin *et al.*, *Cancer Res* **73**, 6856 (Dec 1, 2013).
16. The Cancer Genome Atlas Network*, Nature* **490**, 61 (Oct 4, 2012).
17. M. J. Garnett *et al.*, *Nature* **483**, 570 (Mar 29, 2012).
18. K. E. Weis, K. Ekena, J. A. Thomas, G. Lazennec, B. S. Katzenellenbogen, *Mol Endocrinol* **10**, 1388 (Nov, 1996).

19. J. Baselga *et al.*, *N Engl J Med* **366**, 520 (Feb 9, 2012).

20. Y. Wang, J. B. Trepel, L. M. Neckers, G. Giaccone, *Curr Opin Investig Drugs* **11**, 1466 (Dec, 2010).

21. P. Furet *et al.*, *Bioorg Med Chem Lett* **23**, 3741 (Jul 1, 2013).

22. P. R. Gavine *et al.*, *Cancer Res* **72**, 2045 (Apr 15, 2012).

23. M. Mohammadi *et al.*, *EMBO J* **17**, 5896 (Oct 15, 1998).

24. M. Pollak, *Nat Rev Cancer* **12**, 159 (Mar, 2012).

25. I. Baccelli *et al.*, *Nat Biotechnol* **31**, 539 (Jun, 2013).

26. L. Zhang *et al.*, *Sci Transl Med* **5**, 180ra48 (Apr 10, 2013).

Acknowledgements: We are grateful to all the patients who participated in this study; we thank A. McGovern, C. Hart and the MGH clinical research coordinators for help with clinical studies; P. Spuhler, A. Shah, J. Ciciliano and V. Pai for bioengineering technical support; R. Milano, K. Lynch, H. Robinson, and M. Liebers for technical support; L. Collins (BIDMC) for providing pathological specimens; L. Libby for mouse studies. N. Aceto is a fellow of the Human Frontiers Science Program, the Swiss National Science Foundation, and the Swiss Foundation for Grants in Biology and Medicine. This work was supported by grants from the Breast Cancer Research Foundation (D.A.H), Stand Up to Cancer (D.A.H., M.T., S.M.), the Wellcome Trust (D.A.H., C.B.), National Foundation for Cancer Research (D.A.H.), NIH CA129933 (D.A.H.), NIBIB EB008047 (M.T., D.A.H.), Susan G. Komen for the Cure KG09042 (S.M.), NCI-MGH Proton Federal Share Program (S.M.), the MGH-Johnson and Johnson Center for Excellence in CTCs (M.T., S.M.), and the Howard Hughes Medical Institute (M.Y., D.A.H.).

Fig. 1. *Ex vivo* expansion of breast cancer CTCs.

A. Representative images of non-adherent CTC culture (BRx-07). Top: Phase contrast. Scale bar, 100 μm. Middle: immunofluorescent staining for cytokeratin (CK, red), Ki67 (yellow), CD45 (green), nuclei (DAPI, blue). Scale bar, 20 μm. Bottom: Light microscopic imaging using Papanicolaou staining. Comparable images for uncultured primary CTC are shown in the inserts. Scale bar, 20 μm.

B. Bioluminescent images showing growth of NSG mouse xenografts, following implantation of 20,000 cultured CTCs (BRx-07) into the mammary fat pad (left panel). Quantification of bioluminescent signals for BRx-07-derived mouse xenografts (mean±SD, n=6).

C. Histology of matched primary breast tumors, cultured CTCs and CTC-derived mouse xenografts for two CTC lines. All panels show cellular staining with hematoxylin (blue) and immunohistochemical staining for ER expression (brown). Scale bar, 20 μm.

Fig. 2. Drug sensitivity of cultured CTCs.

Heatmaps representing cell viability following treatment of BRx-07, BRx-68 and BRx-50 CTC lines with selected anti-cancer drugs, either alone or in combination. The presumed driving mutation for each CTC line is noted, and drugs are grouped according to therapeutic class and targeted pathway. For each drug, the range of concentrations tested is centered around the IC_{50} derived from large scale breast cancer cell line screens (*17*), and each concentration represents a 2-fold increase from the previous dose, with each concentration tested in quadruplicate. Drug

concentrations are listed in Table S3. Signal from viable cells remaining after drug treatment is normalized to corresponding vehicle (DMSO)-treated controls, with ratios plotted ranging from red (more viable) to blue (less viable). Drug abbreviation: BYL, BYL719; Fulv, Fulvestrant; Ever, Everolimus; LEE, LEE011; PD, PD0332991; OSI, OSI906; BMS, BMS754807; Tamo, Tamoxifen; Ralo, Raloxifene; Baze, Bazedoxifene; STA, STA9090; Olap, Olaparib.

Fig. 3. Combinatorial drug targeting of mutant *ESR1* and *PIK3CA* in CTC lines.

A. Heatmaps representing cell viability in the BRx-68 CTC line, carrying an *ESR1* mutation (allele frequency 47%), treated with HSP90 inhibitor (STA9090) together with the selective estrogen receptor modulator (SERM) tamoxifen or degrader (SERD) fulvestrant. For these drug combination studies, the concentrations of each drug was varied independently and results are shown in 8 replicates. Cooperative drug interactions are represented by a diagonal gradient, showing increasing cell killing as both drug concentrations increase independently.

B. Downregulation of ER protein expression measured by immunohistochemical staining (brown) of BRx-68 CTC cultures treated for 24 hours with an HSP90 inhibitor (STA9090), versus vehicle (DMSO). Nuclei are stained with hematoxylin. Scale bar, 20 μm. Bar graph shows quantification of percent ER positive cells. More than 200 cells were quantified in each condition.

C. Heatmaps representing cell viability in the BRx-07 line harboring mutations in *PIK3CA* (99% allele frequency) and *FGFR2* (46% allele frequency). Drugs targeting the products of these mutated oncogenic drivers were tested, along with compounds inhibiting non-mutated targets (IGFR and HSP90). Drug combinations shown are: PI3Ki + FGFRi; PIK3Ki + IGFRi; PIK3Ki + HSP90i.

D. Response of BRx-07 CTC-derived mouse xenografts to the PI3K inhibitor BYL719 (n=4), the FGFR2 inhibitor AZD4547 (n=3), the combination of the two inhibitors (BYL719+AZD4547) (n=4), or diluent control (n=4). Mean ± SD. *In vivo* drug administration was initiated following mammary fat pad inoculation with genotyped CTC cultures and establishment of an expanding tumor xenograft, and tumor-derived bioluminescent measurements were normalized to pre-treatment levels.

Table 1. Mutations detected in cultured CTC lines.

Case	Gene	DNA	Protein	Allele[a] Frequency	In pretreatment Tumor[b]	In Multiple CTC Lines	Known Mutation[c]
BRx33[d]	ESR1	A1613G	D538G	0.24	-	-	Br[f], En
	NUMA1	C5501T	S1834L	0.39	-	-	Br
BRx07[d]	TP53	G853A	E285K	0.99	No	-	Bl, Br, Co, HN, Lu
	PIK3CA	A3140T	H1047L	1	No	-	Br, Co, GBM, HN, Ki, Lu, Me, Mel, Ov, En
	FGFR2	T1647A	N549K	0.46	No	-	Br, En
	CDH1	C790T	Q264*	1	Yes	-	Br
	APC	G7225A	G2409R	0.47	Yes	-	Mel
	DGKQ	G2530A	D844N	0.55	-	-	Lu
	MAML2	A2569G	M857V	0.52	-	-	Lu
BRx68	TP53	C1009T	R337C	0.99	No	Yes	Br, Co, HN, Hem, Ov
	ESR1	A1610C	Y537S	0.47	No	Yes	Br[f], En
	PIK3CA	A3140G	H1047R	0.7	Yes	Yes	Br, Co, GBM, HN, Ki, Lu, Me, Mel, Ov, En
	MSN	G1153A	E385K	0.25	-	-	En
BRx50[d]	ESR1	T1607C	L536P	0.06[g]	-	-	Br[f]
	IKZF1	G1444T	G482C	0.09	-	-	Hem
	BRCA2[e]	T6262del	L2039fs	-	-	-	Br (germ line)
BRx42	PIK3CA	G3145C	G1049R	0.60	Yes	Yes	Br, En, Ki
	PIK3CA	C1097G	P366R	0.54	-	-	Br
	KRAS	G35T	G12V	0.99	No	Yes	Br, Co, Hem, Es, GBM, Lu, Ov, En
	IGF1R	G3613A	A1205T	0.06	-	-	Hem
BRx61	TP53	G610T	E204*	0.98	No	Yes	Bl, Br, Ki, Lu, Ov

Footnotes:

a: Mutant allele frequency within oligoclonal cultured CTC populations was calculated as the ratio of mutant sequence reads to total reads for each gene.

b: Where sufficient material was available for analysis, matched archival pretreatment tumor specimens were subjected to Sanger sequencing to confirm selected mutations identified in CTC cultures. Insufficient tumor material is marked (-).

c: List of tumor types reported to harbor the same mutation in pan-cancer (*10*) or COSMIC databases. Abbreviations are: Breast (Br), Endometrial (En), Central_Nervous_System (CNS), Bladder (Bl), Colorectal (Co), Pancreas (Pa), Stomach (St), Head & Neck (HN), Lung (Lu), Thyroid (Th), Glioblastoma (GBM), Kidney (Ki), Prostate (Pr), Medulloblastoma (Me), Melanoma (Mel), Ovarian (Ov), Cervix (Ce), Esophageal (Es), Hematopoietic and Lymphoid tissue (Hem), Sarcoma (Sar), Cholangiocarcinoma (Ch).

d: Cases for which DNA from matched normal tissue was not available.

e: Germline BRCA2 mutation was detected as part of genetic counseling for familial breast cancer.

f: Mutations reported in recent publications (*12-15*).

g: *ESR1* T1607C mutant allele frequency increased to 0.49 after prolonged *in vitro* culture under low estrogen conditions (>6 months).

* Denotes chain termination codon. fs denotes frameshift mutation

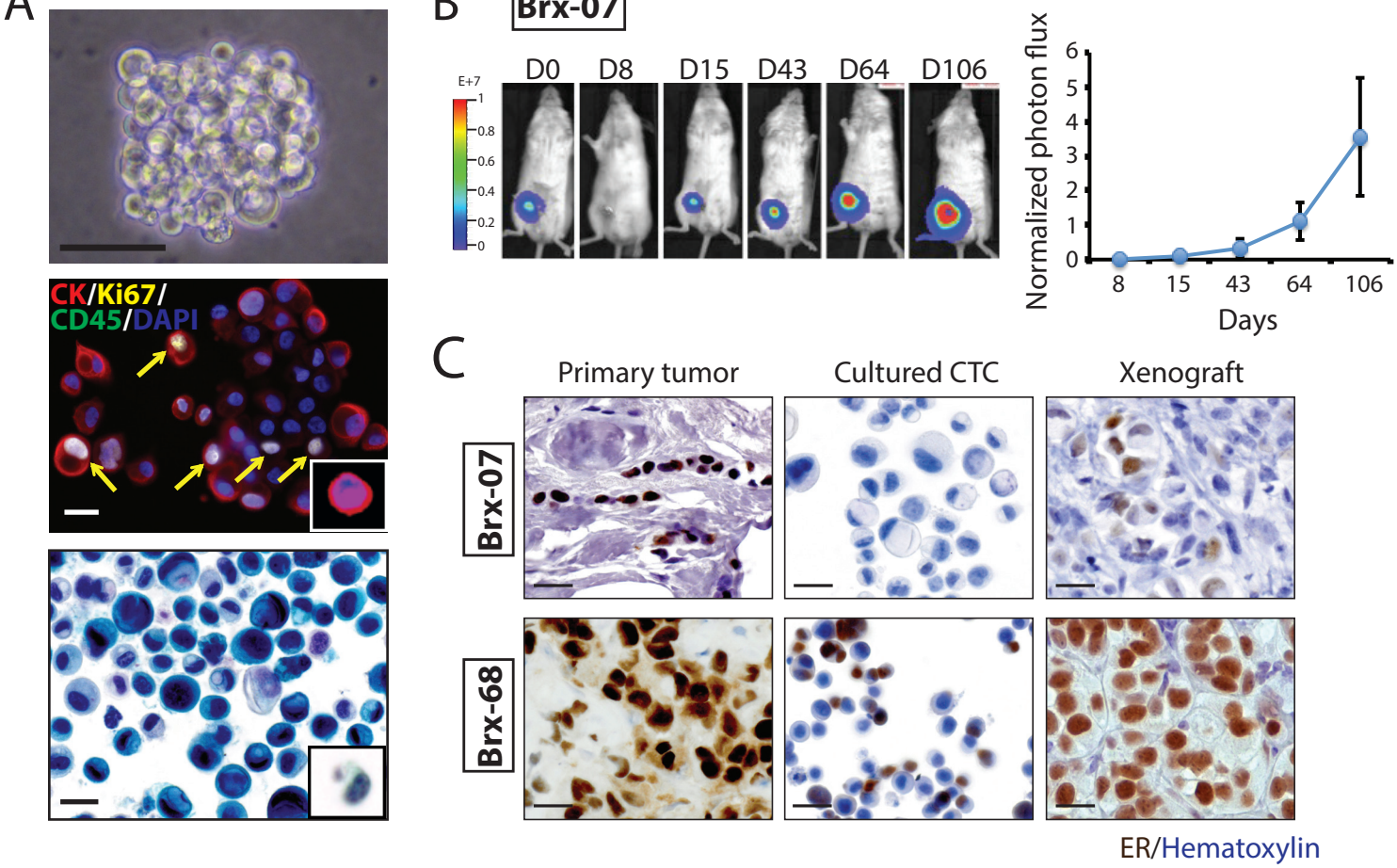
A
CK/Ki67/
CD45/DAPI
B
Brx-07
D0
D8
D15
D43
D64
D106
E+7
1
0.8
0.6
0.4
0.2
0
Normalized photon flux
6
5
4
3
2
1
0
8
15
43
64
106
Days
C
Primary tumor
Cultured CTC
Xenograft
Brx-07
Brx-68
ER/Hematoxylin

Figure 1

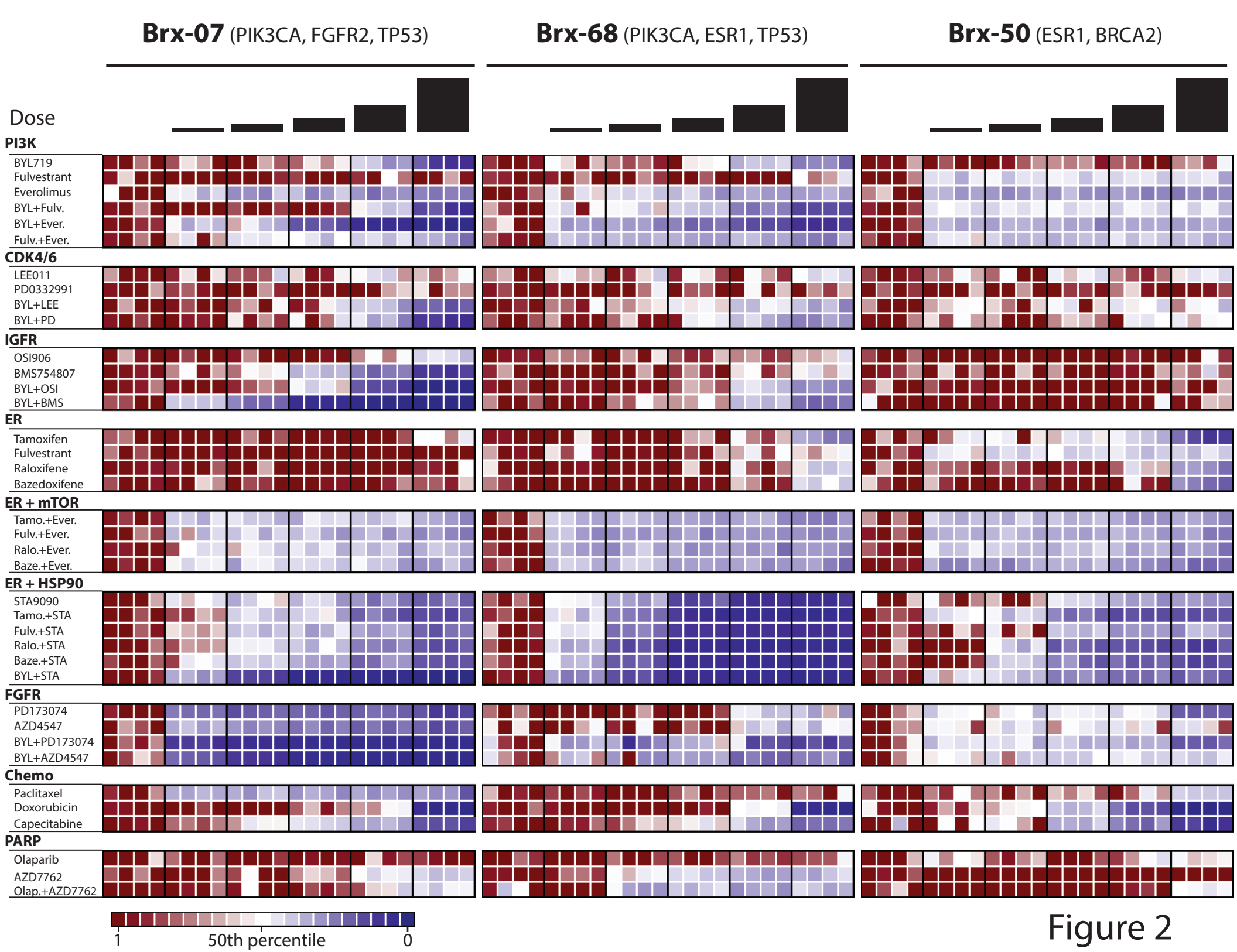
Brx-07 (PIK3CA, FGFR2, TP53)
Brx-68 (PIK3CA, ESR1, TP53)
Brx-50 (ESR1, BRCA2)
Dose
PI3K
BYL719
Fulvestrant
Everolimus
BYL+Fulv.
BYL+Ever.
Fulv.+Ever.
CDK4/6
LEE011
PD0332991
BYL+LEE
BYL+PD
IGFR
OSI906
BMS754807
BYL+OSI
BYL+BMS
ER
Tamoxifen
Fulvestrant
Raloxifene
Bazedoxifene
ER + mTOR
Tamo.+Ever.
Fulv.+Ever.
Ralo.+Ever.
Baze.+Ever.
ER + HSP90
STA9090
Tamo.+STA
Fulv.+STA
Ralo.+STA
Baze.+STA
BYL+STA
FGFR
PD173074
AZD4547
BYL+PD173074
BYL+AZD4547
Chemo
Paclitaxel
Doxorubicin
Capecitabine
PARP
Olaparib
AZD7762
Olap.+AZD7762
1
50th percentile
0

Figure 2

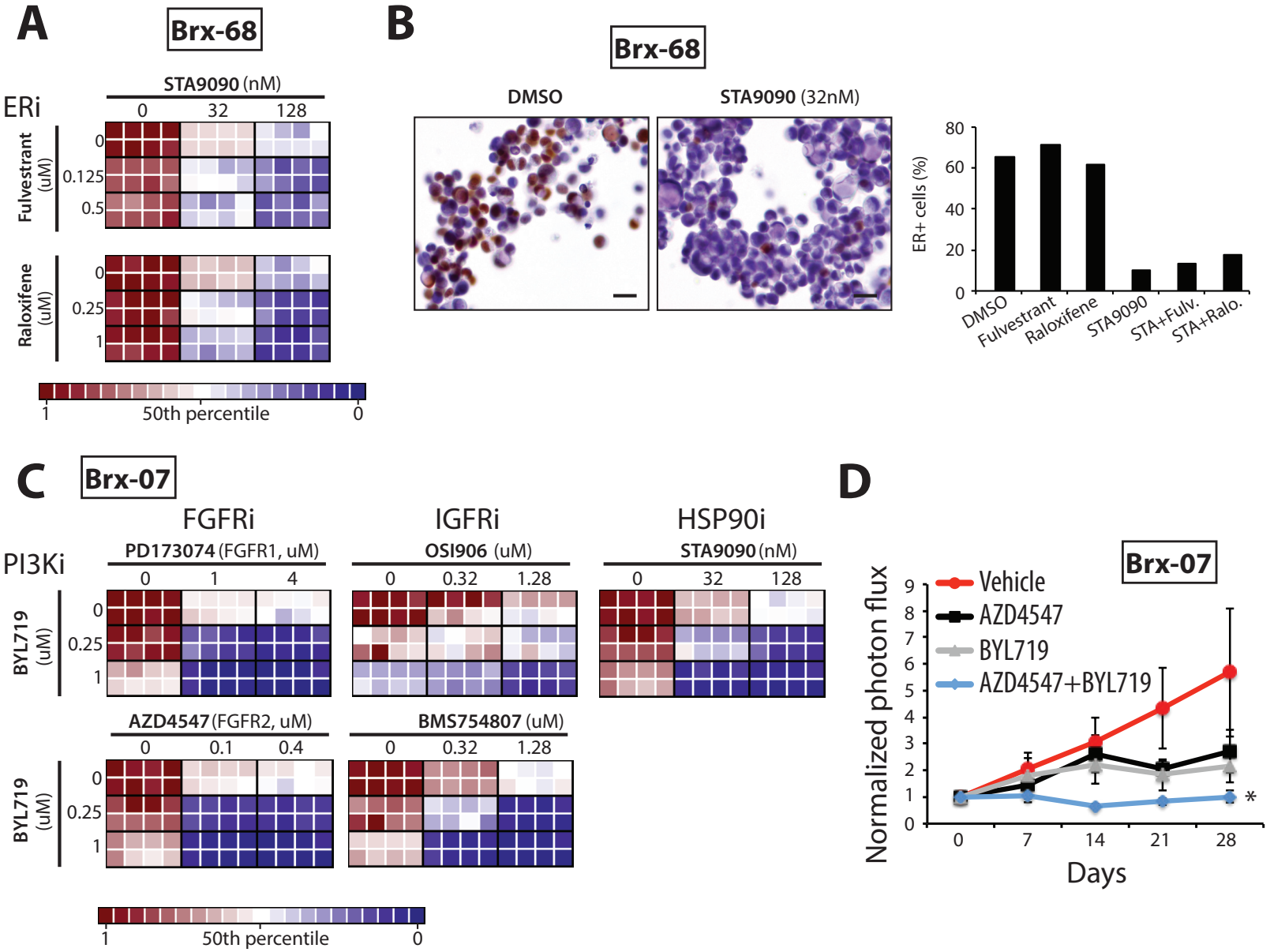
A
Brx-68
STA9090 (nM)
ERi
0
32
128
Fulvestrant (uM)
0
0.125
0.5
Raloxifene (uM)
0
0.25
1
1
50th percentile
0
B
Brx-68
DMSO
STA9090 (32nM)
ER+ cells (%)
80
60
40
20
0
DMSO
Fulvestrant
Raloxifene
STA9090
STA+Fulv.
STA+Ralo.
C
Brx-07
FGFRi
IGFRi
HSP90i
PI3Ki
PD173074 (FGFR1, uM)
0
1
4
OSI906 (uM)
0
0.32
1.28
STA9090 (nM)
0
32
128
BYL719 (uM)
0
0.25
1
AZD4547 (FGFR2, uM)
0
0.1
0.4
BMS754807 (uM)
0
0.32
1.28
BYL719 (uM)
0
0.25
1
1
50th percentile
0
D
Brx-07
Vehicle
AZD4547
BYL719
AZD4547+BYL719
Normalized photon flux
9
8
7
6
5
4
3
2
1
0
*
0
7
14
21
28
Days

Figure 3